The International Journal of Advanced Manufacturing Technology (2018) 96:153–159
https://doi.org/10.1007/s00170-017-1485-5

ORIGINAL ARTICLE

Fabrication and characterization of a bimetallic Al/Cu tube using the tube sinking process

Jalil Salehi[1] · Ahmad Rezaeian[1] · Mohammad Reza Toroghinejad[1]

Received: 2 September 2017 / Accepted: 13 December 2017 / Published online: 19 January 2018

Abstract
In this work, two types of bimetallic tubes were fabricated from aluminum alloy and pure copper using the tube sinking process. The joint quality of the bimetallic tubes was evaluated using the so-called push experiment to determine the bonding shear strength. In addition, different microstructural studies were conducted in order to study the interface character of the layers. It was found that the bonding shear strength of the aluminum-clad copper was slightly higher than that of the copper-clad aluminum. Also, the former exhibited lower bonding shear strength variation than the latter. The discontinuous intermetallic components were detected at the latter interface for both types of bimetallic tubes. Also, it was interesting to note that a relatively thick aluminum oxide layer was found to be formed partially at the copper-clad aluminum tube layer interface. Signs of the cold pressure welding mechanism based on the film theory were indicated in aluminum-clad copper, whereas localized oxidation and wear phenomenon between the aluminum and copper layers deteriorated the bonding strength in copper-clad aluminum.

Keywords Tube sinking · Bimetallic tube · Bond shear strength · Cold pressure welding · Film theory · Tube drawing

1 Introduction

There is a growing demand for bimetallic tubes composed of two distinct metals joined together, introducing interesting combinations of strength, corrosion resistance, and electrical conductivity [1]. For instance, bimetallic tubes such as Al/Cu tubes offer several benefits such as reduced weight and increased corrosion resistance as compared to tubes made purely from copper.

Several methods have been developed to fabricate bimetallic tubes in solid state including rotary swaging [2–4], spin bonding [5], extrusion [6], explosive bonding [7], and high magnetic field bonding [8]. Even though the above methods have been recently developed, more investigations need to be carried out in order to find a simple and industrial process by which bimetallic tubes with suitable surface finish, high dimensional precision, and appropriate bonding are fabricated. Furthermore, in order to produce long products, the production method should be selected accurately. The cold drawing process is one of the methods by which long tubes can be fabricated industrially. It involves the drawing of a tube through a converging die such that its external diameter is reduced, resulting in closer tolerance on the outside diameter and improvement of the surface finish. There are three processes involved in the cold drawing of a tube: hollow drawing, stationary or floating plug drawing, and drawing over a mandrel [9]. In hollow drawing (also known as tube sinking), only the outside diameter of the tube is reduced and the outside surface is subjected to polishing in the die. On the other hand, the wall thickness is not changed significantly with respect to its tolerances.

Although the tube sinking process has been used for quite a long time, its potential in the manufacturing of bimetallic tubes has received little attention and gained few publications. As shown in Fig. 1, it can be assumed that more than one tube is drawn simultaneously by the tube sinking process. As mentioned, the main advantage of the tube sinking process is its capability to produce a long "composite" tube, with high surface quality and high production speed. In this regard, Halaczek

✉ Mohammad Reza Toroghinejad
toroghi@cc.iut.ac.ir

Jalil Salehi
jalil.salehi@ma.iut.ac.ir

Ahmad Rezaeian
a.rezaeian@cc.iut.ac.ir

[1] Department of Materials Engineering, Isfahan University of Technology, Isfahan 84156-83111, Iran

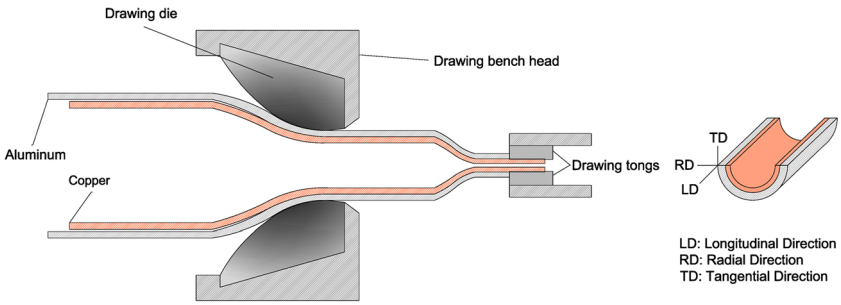

Fig. 1 Schematic depiction of the tube sinking process to fabricate a bimetallic tube

fabricated several kinds of bimetallic tubes from pure copper and brass using tube sinking. He evaluated the deformation behavior of each tube layer and reported that the behavior of the material in the drawing die (in terms of change in thickness) cannot be predictable [10]. However, he did not characterize the interface quality/properties as the main influencing issue in bimetallic products. To our knowledge, no research work has been carried out in order to characterize the bonding mechanism(s) involved in the tube sinking of bimetallic tubes. Therefore, the aim of the present work was initially to produce a bimetallic tube compound of aluminum 6061 and pure copper (as well-known alloys in terms of corrosion resistance and heat conduction properties) to be an excellent replacement for copper tubes in order to save cost and reduce weight. For this purpose, prepared sandwich tubes were drawn simultaneously by the tube sinking process to fabricate aluminum-clad copper and copper-clad aluminum tubes.

2 Experimental procedure

2.1 Materials and process

As-extruded pure copper (OFHC) and aluminum alloy (Al-6061) tubes were selected as the initial materials. Using cold rolling, the tubes' diameters to make a sandwich were sized with the following dimensions (outer diameter/inner diameter):

For aluminum-clad copper: Al tube 16/14 mm, Cu tube 14/12.5 mm
For copper-clad aluminum: Cu tube 16/14 mm, Al tube 14/12 mm

After sizing, the aluminum alloy and copper tubes were annealed at appropriate temperatures, 420 and 450 °C, respectively. In order to remove the oxide layer from the annealed tubes, the pickling process was employed. After pickling, the tubes were subjected to straightening by a straightening machine to remove any distortion caused by the annealing process. The inner surface of the outer tubes, as well as the outer surface of the inner tubes, was then subjected to sandpaper grinding (SiC paper # 320) to create a high level of roughness and to remove the oxide layer. The typical surface textures of the ground copper and aluminum alloy are shown in panels a and b of Fig. 2, respectively. The aluminum alloy and copper tubes were then inserted into each other coaxially to make the tubular sandwich 200 cm in length. It should be mentioned that due to the picking and grinding, a gap of 0.2 mm was created between the tubes. Two types of tubular sandwiches were prepared. For the first type, the aluminum tube was used as the outer layer, called aluminum-clad copper (acc), whereas for the second type, copper was the outer layer, named copper-clad aluminum (cca).

The tube sinking process was performed on a draw bench. To start, one end of the sandwiched tube was reduced to a smaller diameter in order for it to enter the draw die. Then, the jaws gripped the above end of the sandwiched tube to begin the draw operation using oil lubrication. The tubular sandwiches were drawn through a 10-mm-diameter tungsten carbide die, with an entrance angle equal to $2\alpha = 25°$ and a 3.8-mm bearing length. The drawing speed was chosen to be 0.15 m/s. Higher speeds resulted in a temperature rise which could be detrimental in terms of increasing the oxidation rate as well as causing the formation of intermetallic compounds. The latter have been reported to be formed at around 120 °C for a bimetallic joint (Al and Cu) [11]. For the current work, the temperature rise was measured to be 50 and 60 °C for the outer surfaces in acc and cca, respectively. With regard to the above observation, there was no noticeable change in the adhesion quality (shear strength) due to the drawing speed change close to 0.15 m/s.

2.2 Mechanical and microstructural analyses

The push experience was carried out to assess the bonding strength of the fabricated bimetallic tubes using a set of both mandrel and die. The compressive load was applied only on the inner layer. The experience was ended once the compression stroke exceeded 3 mm, while displacement-force data was recorded. The shear strength of the joint was calculated by Eq. (1):

$$\tau_s = \frac{F_{\max}}{A} = \frac{F_{\max}}{\pi dh} \tag{1}$$

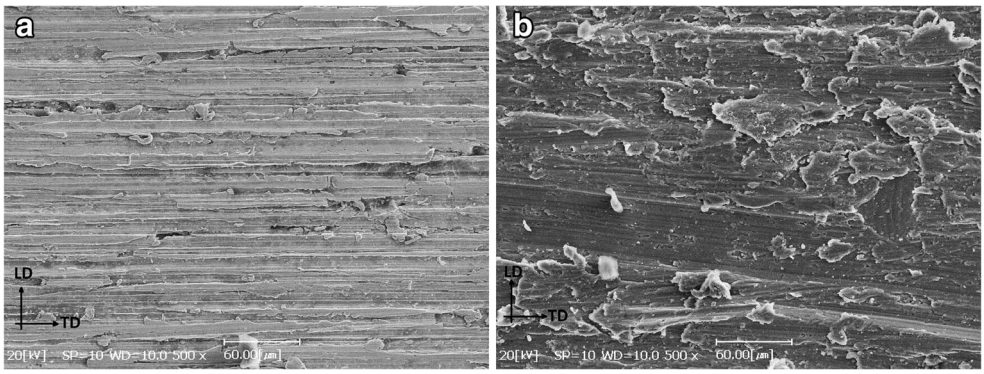

Fig. 2 SEM micrograph of the tube after sandpaper grinding for **a** the inner surface of the copper tube and **b** the outer surface of the aluminum tube

where τ_s is the shear strength, F is the maximum value of force on the inner layer, A is the surface area between the two layers at the interface, d is the outer diameter of the inner layer, h is the specimen height, and π is a constant value equal to 3.14.

Figure 3a shows a typical stress-displacement curve achieved from the push experience. The shear strength was determined as shown by arrows on the curves. It should be mentioned that the experience was repeated on five specimens and the shear strength was reported as the average of the experiences. The experience equipment setup and the tube relocation after the experience are also shown in panels b and c of Fig. 3, respectively.

Tensile tests were carried out on the as-received and as-fabricated tubes according to ASTM E8M. In addition, Vickers hardness tests were done by using a universal hardness tester with a load of 10 kgf. The specimens for Vickers hardness tests were cut from a cross section of the tube (normal to the longitudinal direction of the tube). The average of five measurements for each specimen was reported.

Standard metallography practice was performed on the longitudinal direction (LD)-radial direction (RD) plan (Fig. 1) for each specimen. The specimens were then analyzed using a scanning electron microscope (SEM) equipped with energy-dispersive spectroscopy (EDS). In order to study the surface of the layers at the interface, the specimens were cut in the LD and then the layers were peeled. The inner surface of the outer layer and the outer surface of the inner layer were subjected to the grazing incidence X-ray diffraction (GIXRD) analysis to have a more accurate phase identification.

3 Results and discussion

3.1 Mechanical properties and deformation behavior

Figure 4 shows an image of the as-fabricated acc and cca tubes. As can be seen, both tubes have a smooth and shiny surface finish. It is confirmed that the qualified surface can be achieved by the tube sinking of the bimetallic tube.

The total reduction in area for the acc and cca tubes was 27 and 31%, respectively. It should be mentioned that the reduction in area for the aluminum and copper layers in acc was 24 and 26%, respectively, whereas it was 26 and 38% for cca. Generally, in the cold rolling process of multilayer sheet metals, the softer metal experiences a greater level of deformation than the harder one [12]. However, after the tube sinking process in the present work, the softer tube (i.e., aluminum) exhibited equal or even less deformation as compared to the harder tube (i.e., copper). More investigation is required in order to figure out the above-mentioned result.

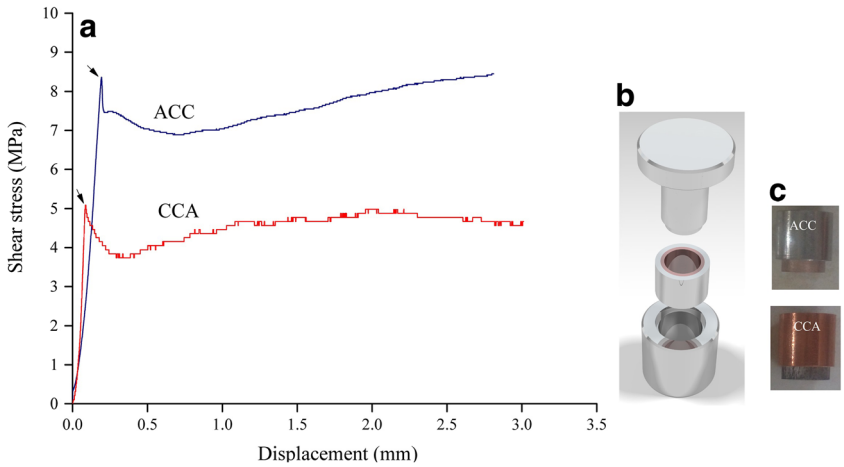

Fig. 3 **a** Stress-displacement graphs after the bimetallic tubes' push experience, **b** push experience setup, **c** specimens after the experience

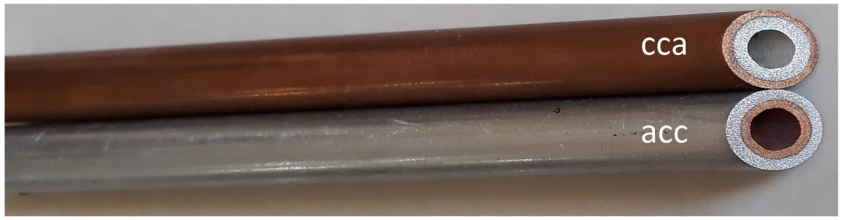

Fig. 4 Photograph of the as-fabricated acc and cca

Figure 5 shows engineering stress-strain curves for aluminum alloy and pure copper used in this work. As shown in Table 1, the values of yield strength and ultimate tensile of the copper tube were higher than those of the aluminum tube.

In addition, both acc and cca showed higher strength than the aluminum and copper, which is related to well-known strain hardening of the tubes during the tube sinking process. Furthermore, the cca tubes exhibited a slightly greater strength since the fraction of copper had a higher strength and a higher strain hardening rate.

The resulting hardness values are presented in Table 1. The initial hardness of the aluminum and copper was 32.4 and 53.1 HV, respectively. After the tube sinking process, it increased to 100 and 110 HV for copper in acc and cca, respectively. As mentioned before, the higher hardness of copper for cca might be related to the higher reduction in area which was 26 and 38% in acc and cca, respectively. On the other hand, the reduction in area for aluminum in acc and cca was 24 and 26%; therefore, the hardness value in the aluminum in both bimetallic tubes was almost 55 HV.

3.2 The joint shear strength

The average of shear strength for acc and cca was determined to be 8.97 ± 0.55 and 7.70 ± 2.07 MPa, respectively. Even though the shear strength of acc was slightly higher than that of cca, the standard deviation for cca was higher than that for acc. The causes of such observation will be explained in detail in Section 3.4. Although there is no information about shear strength for the Al/Cu bimetallic tube fabricated by the tube sinking method as a benchmark, shear strength values for an Al/Cu bimetallic tube manufactured by the equal channel angular pressing (ECAP) process were reported by Ghadimi et al. They reported that after four passes, the shear strength of layers increased from 4.2 to 5.9 MPa [13]. Therefore, it seems that the resulting shear strength from the present work for both acc and cca tubes is comparable with the one that resulted from the severe plastic deformation (SPD) method.

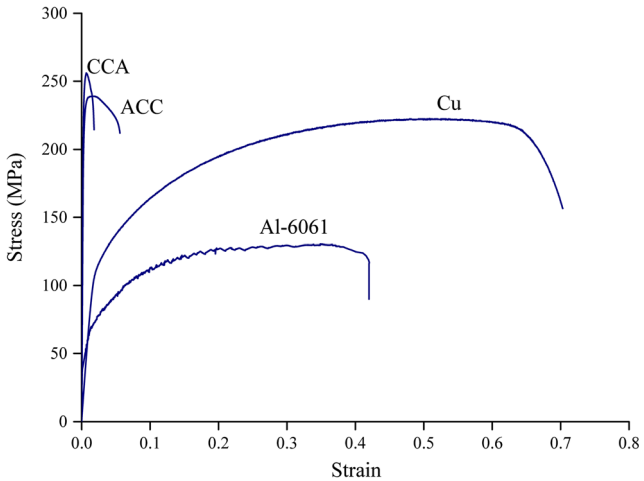

Fig. 5 Engineering stress-strain curve for as-used aluminum alloy, pure copper, acc, and cca

3.3 Microstructural and fracture surface studies

Figure 6a shows the interface microstructures of the Al/Cu joints for acc in the RD-LD plane. As can be seen, the interface is relatively smooth without signs of cracks, holes, crushed particles, or separated layers. Figure 6b, c shows SEM images along with an EDS line scan at the interface close to the intermetallic compound (IMC) location. As can be seen, the concentration of Al and Cu changed smoothly. Some IMC layer approximately 0.7 μm thick was detected to be formed parallel to the interface line. From the EDS results, the IMCs could be identified as Al_2Cu and AlCu considering the atomic ratio (n(Al):n(Cu)) being approximately equal to 2:1 and 1:1, respectively. This was confirmed by the XRD analysis in which the peaks of Al_2Cu for acc were detected. Formation of the IMC can be attributed to the interdiffusion phenomenon that had been taking place between the aluminum and the copper tubes during the sinking process. Furthermore, a thin oxide layer was detected by the EDS line scan (Fig. 6c) close to the aluminum layer, which might be formed as a result of the interfacial interaction during deformation of the layers.

Figure 7a shows the interface microstructures of the Cu/Al joints for cca. As can be seen, the interface of the cca tube was

Table 1 Mechanical properties of the as-used tubes and as-fabricated bimetallic tubes

	Yield strength (MPa)	Tensile strength (MPa)	Hardness (HV)
Aluminum alloy	98	132	32.4
Copper	108	227	53.1
acc (Al/Cu)	211	238	(55/100)
cca (Cu/Al)	238	256	(110/55)

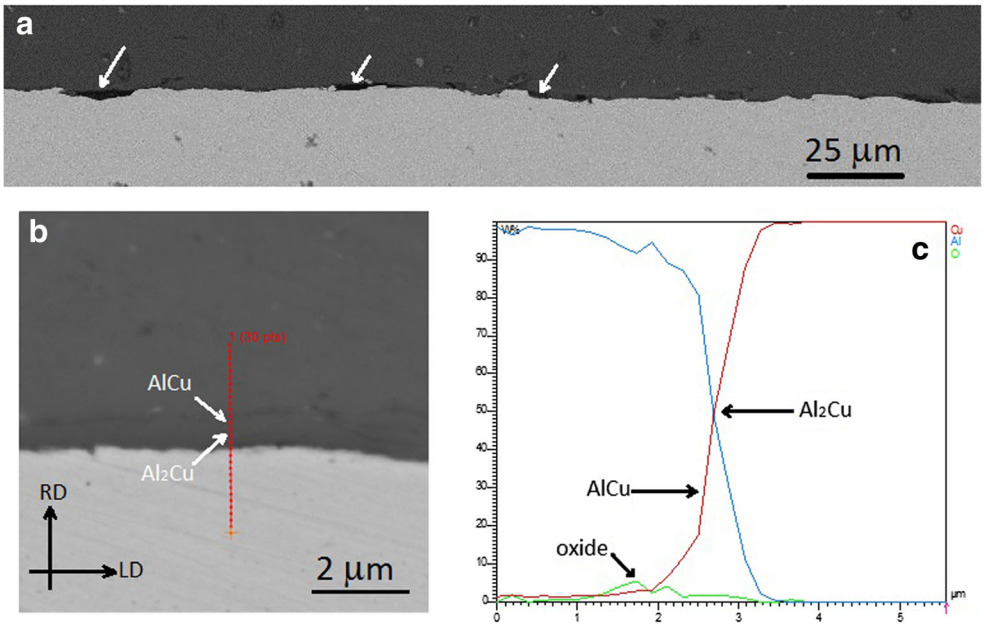

Fig. 6 **a** BSE image of the acc interface from the RD to the LD, **b** and **c** BSE image at higher magnification and EDS line scan from IMC

rougher than that observed for the acc joint. The black areas (shown by arrows) which were located at the interface were analyzed by EDS to be Al_2O_3. Figure 7b, c shows an SEM image along with an EDS line scan that resulted from the above-mentioned interface in another location. As can be seen, there is a thick layer composed of both IMC and Al_2O_3 components. The IMC could be identified as Al_2Cu considering the atomic ratio to be approximately 2:1. It seems that the presence of the Al_2O_3 layer reduced the bond strength mainly due to lack of contact between the two metals. The IMC (Al_2Cu, AlCu) and also Al_2O_3 were recognized by XRD which confirmed the above-mentioned EDS results. In the next section, proposed mechanisms explaining the formation of IMCs and Al_2O_3 will be explained.

3.4 Bonding mechanism

In the tube sinking process, two layers of the metal (the aluminum alloy and pure copper for the current work) are elongated in the drawing direction (DD) while they are under

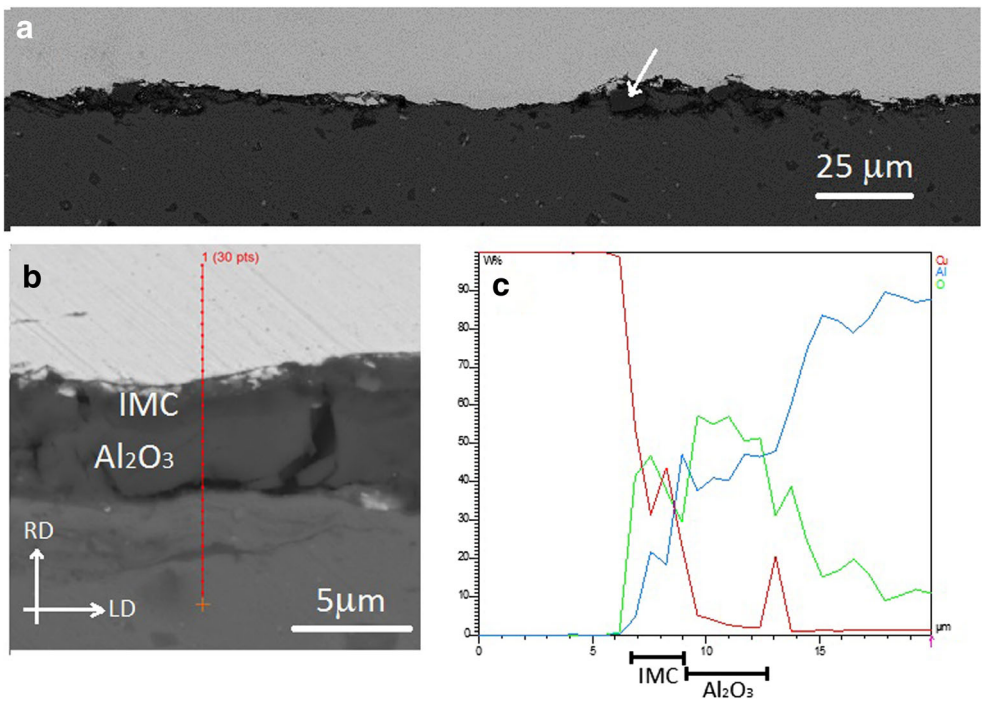

Fig. 7 **a** BSE image of the cca interface from the RD to the LD, **b** and **c** BSE image and EDS line scan from another location at the cca interface

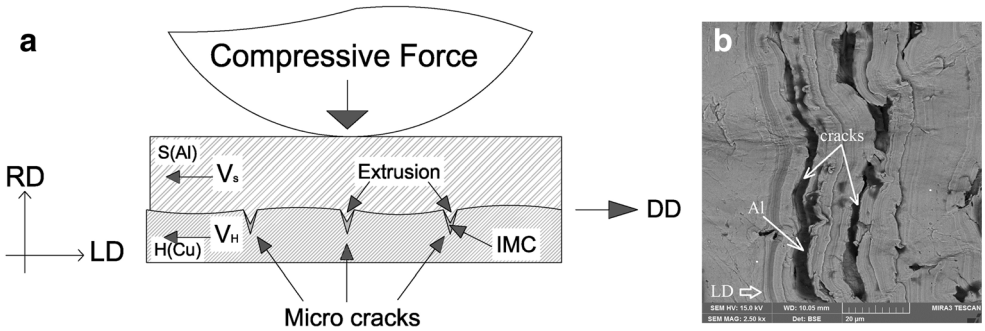

Fig. 8 **a** Schematic image of the cold pressure welding mechanism, **b** BSE image of the copper surface at the interface for the acc specimen

compressive forces applying from the drawing die. In this situation, cold pressure welding might be applied between the two layers at the contact surface. The bonding can be attributed to the well-known mechanisms, i.e., the film theory [14, 15]. As it is well documented, the basic mechanism governing bonding in the cold pressure welding processes based on the film theory is the cracking of the brittle cover layer existing on the surface which can be introduced by scratch brushing, leading to the production of a heavily work-hardened surface layer. After the cracking of the above brittle layer, virgin metal (fresh metal) is extruded through the cracks, resulting in meeting the opposing surface. Figure 8a shows schematically the cracking of the brushed layer caused by surface expansion on harder metal (the copper in the current work) and the filling of these cracks by extrusion of the softer metal (the aluminum in the current work). Such cracks have been formed mostly perpendicular to the LD. Figure 8b shows SEM images of the copper surface at the interface in the acc specimen. As can be seen, the aluminum (black line) is found on the copper surface perpendicularly to the DD (or LD). In fact, the cracks which were formed in the copper side (harder layer) seem to be filled by aluminum (softer layer). It should be mentioned that the authors have not found technical information in the literature in order to compare the results with the ones presented in this paper. However, in a similar process (cold roll bonding process), it was reported that cold rolling of an Al/Cu multilayer sheet from 45 to 66% resulted in fresh metal being extruded within the cracks [16]. This finding confirms the bonding mechanism explained for the present study.

On the other hand, the surface of layers at the interface for the cca tube was found to be different from that for the acc tube. Figure 9a shows a schematic image proposed to explain the interaction of the layers because of different deformation flows (V) for the copper as the hard layer (H) and the aluminum alloy as the soft layer (S). Interaction of the surface at the interface which is shown by arrows in Fig. 9a may cause a wear phenomenon between the contact asperities. The wear could, in turn, result in a temperature rise at the interface, leading to fragmentation of the work-hardened surface layer and the adhering of the soft metal to the hard metal surface, so-called adhesion wear. The latter could, in turn, cause either the adhered soft metal (aluminum) to react with the hard metal (copper) or the reaction of the active metal (i.e., aluminum) with existent oxygen in an air gap, as indicated in Fig. 9a.

Figure 9b shows an SEM image of the copper surface at the interface for the cca. Black points were observed to be distributed on the copper surface. It was shown that the points consist of Al_2O_3 using EDS analysis. In addition, small particles of the copper (shown as point F in Fig. 9b) were detected to be distributed on the surface which could be attributed to fragmentation of the hardened copper layer.

In acc, by applying a compression force from the die on the outer surface, soft aluminum extrudes to the cracks which was formed in the copper side; thus, the cold welding based on the film theory and energy barrier theory was the dominant bonding mechanism. In cca, however, non-intimate contact followed by severe interaction between layers caused oxide

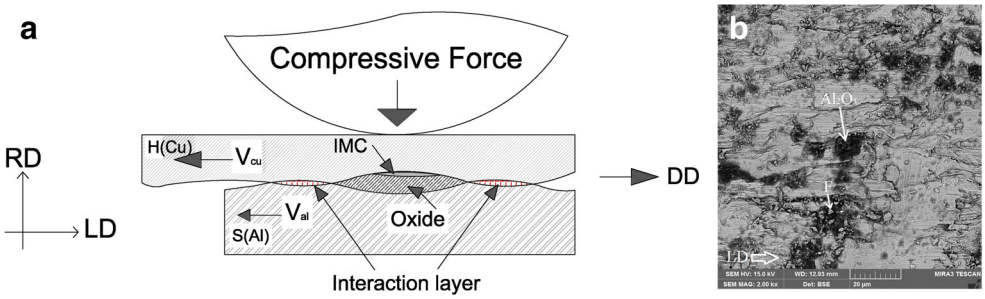

Fig. 9 **a**Schematic image of the proposed mechanism that occurred at the interface in cca, **b** BSE image of copper at the interface for the cca specimen

(Al_2O_3) generation at the interface. Therefore, as explained in Section 3.2, the cca has shown a lower shear strength with respect to acc. Furthermore, in cca, the copper can flow on the relatively softer substrate (i.e., aluminum alloy) in the RD. Therefore, the copper tube could come in contact partly with the aluminum substrate, whereas the rest of the tube might be delaminated, leading to the creation of air gaps at the interface. As previously mentioned, as temperature increases (due to pressure and interfacial sliding), an oxide layer might be formed within the air gaps. Therefore, an inhomogeneous interface, partly covered by oxide (Fig. 7a, b), is expected to be formed in cca. Accordingly, depending on features of the sample selected for the push test, the shear strength can be varied. It should be mentioned that the above observation was examined several times; therefore, the inhomogeneity and higher standard deviation were reported for the cca interfaces. In addition, the reduction in shear strength of the cca could be attributed to possible flaking of the oxide layer at the Cu/Al interface. This can be a random phenomenon resulting in uncertainty in the shear strength values of the cca.

4 Conclusions

In this study, Al/Cu bimetallic tubes with two different stacking sequences were fabricated using the tube sinking process. The results of the investigation can be summarized into the following conclusions:

1. The bonding shear strength of the aluminum-clad copper was slightly higher than that of the copper-clad aluminum. But, the former exhibited lower bonding shear strength fluctuation than the latter.
2. The discontinuous intermetallic components (Al_2Cu and AlCu) were detected at the interface for both bimetallic tubes. Furthermore, a relatively thick aluminum oxide layer was found to be formed at some parts of the copper-clad aluminum layer interface.
3. The signs of the cold pressure welding mechanism based on the film theory and energy barrier theory were indicated in aluminum-clad copper, whereas localized oxidation and wear phenomenon between aluminum and copper layers deteriorated bonding strength in the copper-clad aluminum.

References

1. Ashby MF (2005) Materials selection in mechanical design, 3rd edn. Butterworth-Heinemann, Oxford
2. Kocich R, Macháčková A, Kunčická L, Fojtík F (2015) Fabrication and characterization of cold-swaged multilayered Al–Cu clad composites. Mater Des 71:36–47. https://doi.org/10.1016/j.matdes.2015.01.008
3. Zhang Q, Zhang Y, Cao M, Ben N, Ma X, Ma H (2017) Joining process for copper and aluminum tubes by rotary swaging method. Int J Adv Manuf Technol 89(1-4):163–173. https://doi.org/10.1007/s00170-016-8994-5
4. Zhang Q, Jin K, Mu D (2014) Tube/tube joining technology by using rotary swaging forming method. J Mater Process Technol 214(10):2085–2094. https://doi.org/10.1016/j.jmatprotec.2014.02.002
5. Mohebbi MS, Akbarzadeh A (2011) Fabrication of copper/aluminum composite tubes by spin-bonding process: experiments and modeling. Int J Adv Manuf Technol 54(9-12):1043–1055. https://doi.org/10.1007/s00170-010-3016-5
6. Park HJ, Na KH, Cho NS, Lee YS, Kim SW (1997) A study of the hydrostatic extrusion of copper-clad aluminum tube. J Mater Process Technol 67(1-3):24–28. https://doi.org/10.1016/S0924-0136(96)02812-9
7. Guo X, Wang H, Liu Z, Wang L, Ma F, Tao J (2016) Interface and performance of CLAM steel/aluminum clad tube prepared by explosive bonding method. Int J Adv Manuf Tech 82(1-4):543–548. https://doi.org/10.1007/s00170-015-7380-z
8. Truog AG (2012) Bond improvement of Al/Cu joints created by very high power ultrasonic additive manufacturing. Dissertation, The Ohio State University
9. Dieter GE (1986) Mechanical metallurgy, 3rd edn. Mc Graw-Hill Book Co., New York
10. Halaczek D (2016) Analysis of manufacturing bimetallic tubes by the cold drawing process. Metall Mater 61(1):241–248
11. Abbasi M, Karimi Taherib A, Salehi MT (2001) Growth rate of intermetallic compounds in Al/Cu bimetal produced by cold roll welding process. J Alloys Compd 319(1-2):233–241. https://doi.org/10.1016/S0925-8388(01)00872-6
12. Chi Tseng H, Hung C, Chuan Huang C (2010) An analysis of the formability of aluminum/copper clad metals with different thicknesses by the finite element method and experiment. Int J Adv Manuf Tech 49(9-12):1029–1036. https://doi.org/10.1007/s00170-009-2446-4
13. Ghadimi S, Sedighi M, Djavanroodi F, Asgari A (2015) Experimental and numerical investigation of a Cu–Al bimetallic tube produced by ECAP. Mater Manuf Process 30(10):1256–1261. https://doi.org/10.1080/10426914.2014.984210
14. Bey N (1986) Cold welding. Part I: characteristic, bonding mechanism, bond strength, metal. Construction 18:369–372
15. Li L, Nagai K, Yin F (2008) Progress in cold roll bonding of metals. Sci Technol Adv Mater 9(2):023001. https://doi.org/10.1088/1468-6996/9/2/023001
16. Chen CY, Chen HL, Hwang WS (2006) Influence of interfacial structure development on the fracture mechanism and bond strength of aluminum/copper bimetal plate. Mater Trans 47(4):1232–1239. https://doi.org/10.2320/matertrans.47.1232